

A novel mechanism of charge density wave in a transition metal dichalcogenide

D. W. Shen¹, B. P. Xie¹, J. F. Zhao¹, L. X. Yang¹, L. Fang²,
J. Shi³, R. H. He⁴, D. H. Lu⁴, H. H. Wen², and D.L. Feng^{1*}

¹Department of Physics, Applied Surface Physics State Key Laboratory, Fudan University, Shanghai 200433, China

²National Lab for Superconductivity, Institute of Physics and National Lab for Condensed Matter Physics, Chinese Academy of Sciences, P.O. Box 603, Beijing 100080, P. R. China

³School of Physics, Wuhan University, Wuhan, 430072, P. R. China and

⁴Department of Applied Physics and Stanford Synchrotron Radiation Laboratory, Stanford University, Stanford, CA 94305, USA

(Dated: September 28, 2018)

Charge density wave, or CDW, is usually associated with Fermi surfaces nesting. We here report a new CDW mechanism discovered in a $2H$ -structured transition metal dichalcogenide, where the two essential ingredients of CDW are realized in very anomalous ways due to the strong-coupling nature of the electronic structure. Namely, the CDW gap is only partially open, and charge density wavevector match is fulfilled through participation of states of the large Fermi patch, while the straight FS sections have secondary or negligible contributions.

PACS numbers: 71.18.+y, 71.45.Lr, 79.60.-i

It has been a standard textbook-example that charge density wave (CDW), one of the main forms of ordering in solid, is mostly associated with nesting Fermi surface (FS) sections. In charge ordered materials ranging from one-dimensional (1D) (TaSe₄)₂I and blue bronze[1, 2] to two-dimensional (2D) manganites, and from surface reconstruction in weak correlated metals to checker board pattern of strongly correlated high temperature superconductors[3, 4], the charge fluctuations associated with the ordering wave vector scatter the electrons between two nested FS sections and effectively drive the system into an ordered ground state. However, this classical picture failed in the very first 2D CDW compound discovered in 1974, *i.e.* the transition metal dichalcogenides (TMD's)[5]. The $2H$ -structured TMD's have a hexagonal lattice structure, and in its CDW phase, a 3×3 superlattice forms[5, 6]. It was found that the ordering wavevectors do not match the nested FS sections, and generally no CDW energy gap was observed at the FS[7, 8]. After decades of continuous effort, the origin of CDW for the $2H$ -structured TMD's has been a long standing mystery. As a result, the subtle details of the competition and coexistence of CDW and superconductivity in TMD's[9] remain to be revealed[10].

In this letter, we studied the electronic origin of the CDW in a $2H$ -TMD, $2H$ -Na_{*x*}TaS₂, by angle-resolved photoemission spectroscopy (ARPES). The CDW mechanism in this material was discovered after the revelation of the following exotic properties. i) The electronic structure exhibits strong coupling nature, with finite density of states at the Fermi energy(E_F) over almost the entire Brillouin zone(BZ), forming so-called Fermi patches. ii) In the CDW state, only a fraction of the states at E_F is gapped. iii) The density of states near E_F directly correlates with the ordering strength. iv) Fermi patch, instead of Fermi surface, is relevant for CDW. We show that this new "Fermi-patch mechanism" for CDW is rooted in the

strong coupling nature of the electronic structure and it may be a general theme of ordering in the strong coupling regime of various models, and applicable to systems with similar electronic structure.

For the systematic studies of the electronic structure in a $2H$ -TMD compound, $2H$ -Na_{*x*}TaS₂ with 2%, 5% and 10% Na concentration were synthesized with CDW transition temperature T_{CDW} 's are 68K, 65K and 0K respectively. The samples are labelled as CDW^{68K}, CDW^{65K}, and CDW^{0K} hereafter. The corresponding superconducting transition temperatures are 1.0K, 2.3K and 4.0K respectively, a manifestation of the competition between CDW and superconductivity in this system. The data were mainly collected using 21.2eV Helium-I line of a discharge lamp combined with a Scienta R4000 analyzer, and partial measurements were carried out on beam line 5-4 of SSRL. The overall energy resolution is 8 *meV*, and the angular resolution is 0.3 degrees.

Photoemission spectra taken on samples with (CDW^{65K}) and without CDW (CDW^{0K}) are compared in Fig. 1a-d. In both cases, the spectral lineshapes are remarkably broad, and no quasiparticle peaks in the conventional sense are observed. The large linewidth is of the same order as the dispersion, which clearly indicates the incoherent nature of the spectrum and the system is in the *strong coupling* regime. Taking the normalized spectra at \mathbf{M} as reference[12], spectra at Γ , \mathbf{K} , and the Fermi crossing of the Γ - \mathbf{M} cut are compared in Fig. 1e. The difference between CDW^{0K} and CDW^{65K} is striking. Although they have similar density of states at the Fermi crossing area, for momentum regions away from the FS, CDW^{65K} has much stronger spectral weight than CDW^{0K}, no matter whether it is inside the occupied region (\mathbf{M} point), or in the unoccupied region (Γ and \mathbf{K} points) in the band structure calculations[13]. Particularly, one finds that even when the spectral centroid is well below E_F ,

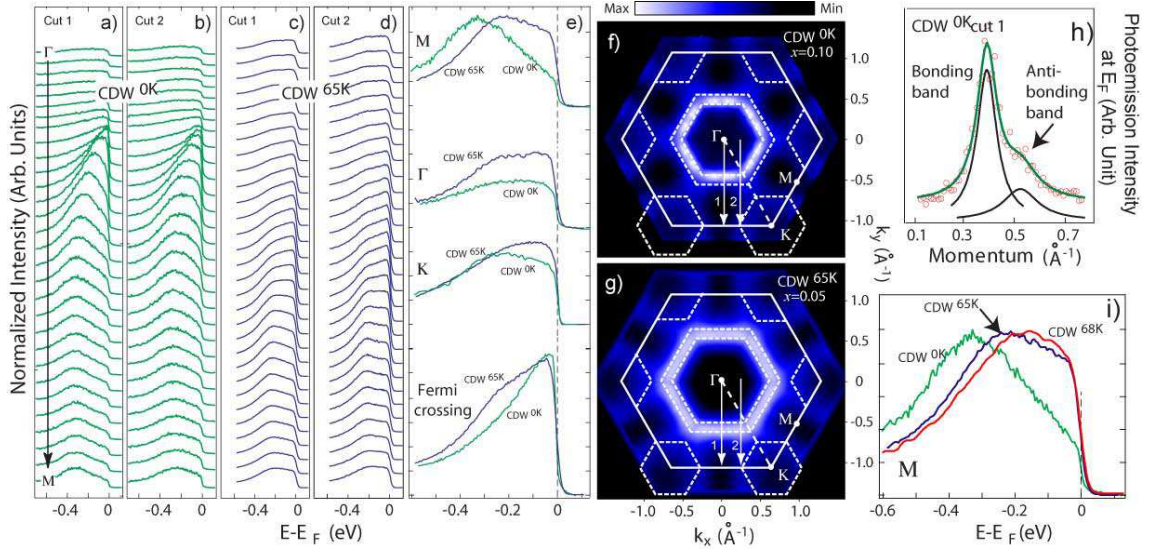


FIG. 1: Typical ARPES spectra for **a-b**, CDW^{0K} at $T=15K$ and **c-d**, CDW^{65K} at $T=95K$ respectively along the marked cuts in the Brillouin zone in panels **f** and **g**. **e**, Comparison of photoemission spectra for different $2H-Na_xTaS_2$'s at high symmetry points M , Γ , K and at the Fermi crossing of cut1. **f** and **g**, The photoemission intensity integrated within $10meV$ of E_F is shown for CDW^{0K} and CDW^{65K} respectively. (Both data were taken at $15K$ and the image was 6-fold symmetrized.) The Fermi surfaces are marked by dashed lines, where the antibonding and bonding bands could be resolved for the Γ pockets in the momentum distribution curve (one example is shown in **h** for CDW^{0K}).

the finite residual weight at E_F beyond background exists around M . We note that the CDW^{0K} sample has higher Na doping than CDW^{65K} , yet its lineshape is generally sharper. Therefore, disorder effects induced by the dopants should be negligible. The residual weight observed near E_F thus should be associated with the intrinsic strong coupling nature of the system, which (within several $k_B T_{CDW}$ around E_F) shows a monotonic correlation with T_{CDW} in Fig. 1i.

Although the spectra are broad, Fermi surfaces could still be defined as the local maximum of the spectral weight at E_F [14], which are plotted in Fig. 1f-g for CDW^{0K} and CDW^{65K} respectively. Three FS pockets can be identified through the momentum distribution curve analysis: two hole pockets around Γ , as exemplified in Fig. 1h, and one hole pocket around K . Bilayer band splitting of the two TaS_2 layers in a unit cell manifests itself as the inner and outer Gamma pockets, while the splitting of the K pockets is indistinguishable. The FS volumes are evaluated to be 1.05 ± 0.01 and 1.11 ± 0.01 electrons per layer for the 5% and 10% Na doped Na_xTaS_2 samples respectively, consistent with the nominal dopant concentrations. This resembles the high temperature superconductors, where the Fermi surfaces defined in this conventional way are consistent with the band structure calculations and follow the Luttinger sum rule quite well[15], yet there are large Fermi patches near the antinodal regions[16]. In CDW^{65K} case, almost the entire BZ appear to be one gigantic Fermi patch. However, so far, searches for the CDW mechanism are mostly centered on the Fermi surfaces, not the Fermi patch.

The differences between CDW^{65K} and CDW^{0K} spec-

tra in the Fermi patch region(Fig.1e) are intriguing. Fig. 2a-b show spectra taken from M at different temperatures for CDW^{65K} and CDW^{0K} respectively. While the CDW^{0K} spectra simply exhibit a clear Fermi crossing and thermal broadening, the CDW^{65K} spectra appear very anomalous. Take the spectrum at $7K$ as an example, while the upper part of the spectrum is suppressed to higher binding energies, the middle point of the leading edge of the lower part still matches E_F . There is an apparent turning point between these two parts of the spectrum. By dividing the spectra with the corresponding finite temperature Fermi-Dirac distribution functions, in Fig. 2c, one clearly observes that about 29% of the spectral weight at E_F has been suppressed for CDW^{65K} . An energy gap has opened on part of the states here, which is estimated to be $\sim 35meV$ based on the middle point of the leading edge. Contrastively, there is no sign of gap opening for CDW^{0K} (Fig. 2d).

It was recently suggested by Barnett and coworkers[17] that a $2H-TMD$ system is decoupled into three sub-lattices. While one of the sub-lattices is undistorted and gapless below T_{CDW} , the other two are gapped at the FS. For CDW^{65K} , similar behavior is observed except that gap does not open at Fermi Surface and just about $1/3$ of the spectrum is gapped. *Phenomenologically*, one can decompose the spectra into gapped and ungapped components. The ungapped component is simulated as

$$A_u(k, \omega, T) = \alpha A(k, \omega, 85K) \frac{f(\omega, T)}{f(\omega, 85K)}$$

, where $A(k, \omega, T)$ is the spectral function, $f(\omega, T)$ is the resolution convoluted finite temperature Fermi-Dirac dis-

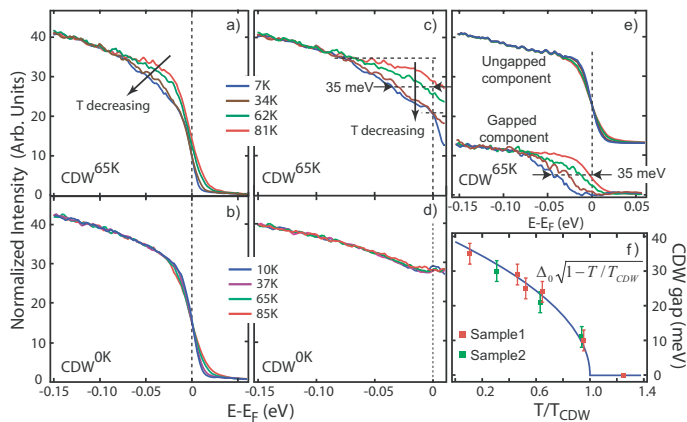


FIG. 2: The CDW gap measurements of $2H\text{-Na}_x\text{TaS}_2$. ARPES spectra taken at \mathbf{M} for different temperatures **a**, CDW^{65K} and **b**, CDW^{0K} . **c-d**, The spectra in **a** and **b** divided by the resolution convoluted Fermi-Dirac distribution at the corresponding temperatures. **e**, Each spectrum in **a** is decomposed into a gapped component and an ungapped component. **f**, The temperature dependence of the CDW gap. The solid line is the fit to a mean field formula, $\Delta_0 \sqrt{1 - \frac{T}{T_{CDW}}}$.

tribution function, and $\alpha = 0.71$. The gapped components

$$A_g(k, \omega, T) = A(k, \omega, T) - A_u(k, \omega, T)$$

The decomposition of spectra in Fig. 2a is shown in Fig. 2e, where the ungapped components exhibit the same behavior as in the CDW^{0K} spectrum, and the gapped components clearly reveal a clean energy gap of about 35meV at 7K. We emphasize that although the decomposition method is adopted hereafter, all the qualitative results can be obtained through the conventional method in Fig. 2c as well. The temperature evolution of the gap is shown in Fig. 2f for two different CDW^{65K} samples. Interestingly, the gap does not saturate at low temperature, and it can be fitted very well to $\Delta_0 \sqrt{1 - \frac{T}{T_{CDW}}}$, which is the mean field theory form at temperature close to T_{CDW} [18]. Here the fitted $\Delta_0 \sim 39\text{meV} \sim 6k_B \cdot T_{CDW}$.

Spectra at other momenta could be decomposed in the same way quite robustly[19], and the CDW gap was mapped over the entire Brillouin zone for CDW^{65K} (Fig. 3a). Strikingly, finite CDW gap exists over most of the Brillouin zone. Its maximum locates around \mathbf{M} , and no gap is observed around the inner Γ Fermi pocket and within. Noticeably, the gap is finite in the \mathbf{K} Fermi pockets, as there is finite spectral weight at E_F . Close comparisons of spectra at various momenta are shown in Fig. 3b-d. In between \mathbf{M} and the Fermi crossing (Fig. 3b), the upper part of the low temperature spectrum is overlaid with the normal state spectrum, which is a sign of gap opening. In Fig. 3c, for spectrum at the inner Γ Fermi pocket, no sign of gap opening is observed, consistent with previous studies[7, 8]. Fig. 3d illustrates

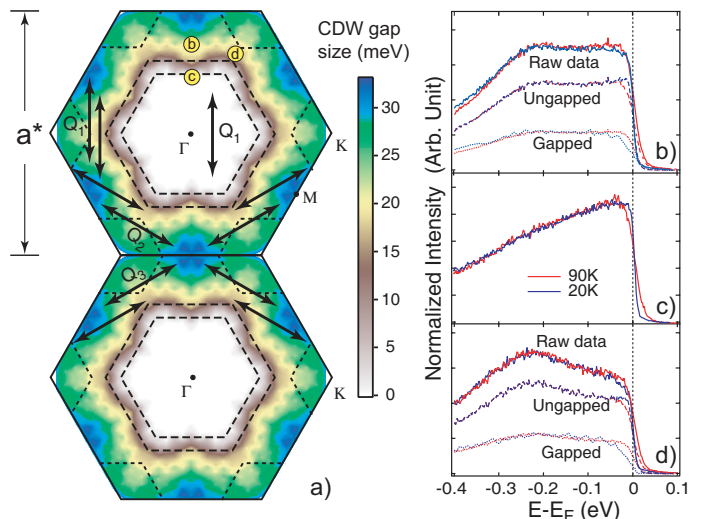


FIG. 3: The gap map over the Brillouin zone. **a**, The false color plot of the CDW gap in the first Brillouin zone of CDW^{65K} , where the dashed lines indicate the Fermi surfaces. States in the gapped region could be connected by the CDW wavevectors, \mathbf{Q}_i ($i=1,2,3$), as indicated by the double-head arrows. **b-d**, Comparison of the typical spectra in normal and CDW state at various momenta marked by the circled letters in **a**. The gapped spectra are decomposed into ungapped (dashed lines) and gapped portion (dotted lines).

that a gap of 15meV is observed at the saddle point of the band calculation. An alternative mechanism was proposed for $2H\text{-TMD}$'s involving the scattering between saddle points, which would cause a singularity in density of states, and thus an anomaly in the dielectric response function[20]. The gap near this point has been reported before[21], but the distance between these points do not match the CDW ordering wavevectors[22, 23]. In the current gap map, nothing abnormal is observed for this momentum.

The CDW in TMD's is associated with structural transitions[5, 6], therefore, electron-phonon interactions are also crucial in the problem. Since the low energy electronic structure of $2H\text{-Na}_x\text{TaS}_2$ is dominated by the Ta 5d electrons [13], among which Coulomb interactions are usually weak, the broad ARPES lineshape would suggest strong electron-phonon interactions. A kink in the dispersion corresponding to the phonon energy scale was found for $2H\text{-Na}_x\text{TaS}_2$ (not shown here) as in other $2H\text{-TMD}$ compounds[24]. In this context, the anisotropic gap distribution might be attributed to the anisotropy of electron-phonon couplings [25, 26], and states in the ungapped region simply may not couple with the relevant phonons. One critical requirement, *i.e.* states in different gapped regions need to be coupled by phonons with the CDW wavevectors, can now be fulfilled in the gap map, as illustrated by the arrows in Fig. 3a. $\mathbf{Q}_i = \mathbf{a}_i^*/3$, ($i=1,2,3$) here are the CDW wavevectors, \mathbf{a}_i^* 's being the reciprocal lattice vectors along the three $\Gamma\text{-M}$ directions. This also explains why the size

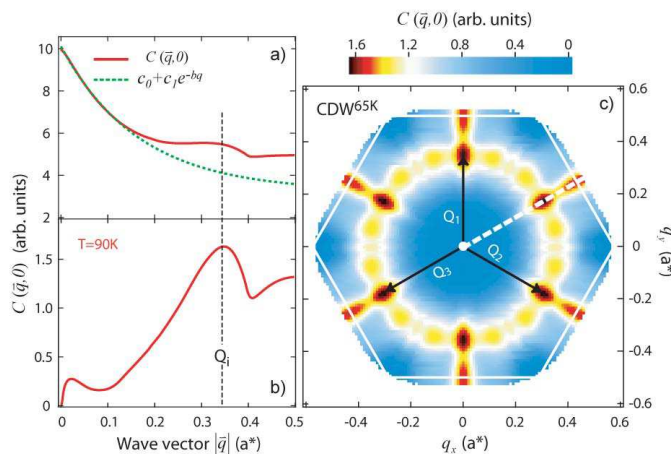


FIG. 4: **a** Autocorrelation of the ARPES intensity at E_F in the normal state of CDW^{65K} for wavevector along the Γ -M direction. The dashed line is an exponential decay plus a constant, which is deduced in **b** to highlight the structure. **c** The partial autocorrelation in the 2D momentum transfer space obtained in the same way as in **b**. Repeated zone scheme is taken in the integration, and thus $C(\vec{q}, 0)$ is symmetric with respect to the boundaries (white hexagon).

of the Fermi surfaces can vary significantly for different 2H-TMD systems, with nearly system-independent CDW ordering wavevectors[22, 23, 27].

One open question in the above picture is that charge fluctuations with other wavevectors are also allowed, and it is not obvious why \mathbf{Q}_i 's are special. For cuprate superconductors, it has been demonstrated that the autocorrelation of ARPES spectra,

$$C(\vec{q}, \omega) \equiv \int A(\vec{k}, \omega) A(\vec{k} + \vec{q}, \omega) d\vec{k}$$

, could give a reasonable count for the charge modulations observed by STM[28, 29]. This joint density-of-states describes the phase space for scattering of electrons from the state at \vec{k} to the state at $\vec{k} + \vec{q}$ by certain modes with wavevector \vec{q} . Therefore, one would expect that it peaks at the ordering wavevector for $\omega = 0$ near the phase transition of static order. Since the states in the gapped Fermi patch are responsible for the CDW here, autocorrelation analysis is conducted in the normal state to study the CDW instabilities of CDW^{65K} over regions that would be gapped below T_{CDW} . The resulting $C(\vec{q}, 0)$ is shown in Fig. 4a for \vec{q} along the Γ -M direction, which is mainly consisted of a component at $\vec{q} = 0$ that exponentially decays, and several features in Fig. 4b, where a peak is clearly observed around the CDW ordering wavevector. The peak at $\vec{q} = 0$ would require coupling to very long wavelength phonons, which presumably is very weak. Consistently, a recent calculation has shown that an optical phonon branch softens significantly around \mathbf{Q}_i , and no sign of softening is observed at $\vec{q} = 0$ [30]. In the 2D partial $C(\vec{q}, 0)$ map (obtained after deducting the exponential decaying part and

the constant background) in Fig. 4c, although there are a few local maxima corresponding to various possible orderings, the highest peaks are those at \mathbf{Q}_i . Therefore, our results suggest that the electronic structure is in favor of the charge instability at \mathbf{Q}_i 's, and eventually the system becomes unstable to the CDW formation below T_{CDW} in collaboration with the phonons. Furthermore, it is also consistent with the positive correlation between the spectral weight near E_F and T_{CDW} in Fig. 1i.

The competition and coexistence of CDW and superconductivity can be understood within the new framework. Recent photoemission studies have revealed that superconducting gap opens at the \mathbf{K} and Γ pockets[10, 25]. The CDW gap opens at a temperature higher than the superconducting transition, but it just partially suppresses the density of states around the \mathbf{K} pocket and outer Γ pocket. Therefore, as observed in most 2H-TMD's, superconductivity is suppressed but not eliminated by the CDW.

To summarize, the Fermi-patch mechanism of CDW in 2H- Na_xTaS_2 is characterized by the realization of both ingredients of the CDW, energy gap and wavevector match on the Fermi patches. Unlike other CDW mechanisms based on band structure effects, it is rooted in the strong-coupling nature of its electronic structure, which provides phase space needed for CDW fluctuations. Furthermore, this mechanism would be realized not only in polaronic systems, but also in materials where strong electron correlations could cause Fermi patches, and thus CDW instabilities.

We thank Profs. H. Q. Lin, J. L. Wang, Q. H. Wang, J. X. Li, Z. D. Wang and F. C. Zhang for helpful discussions. This work is supported by NSFC, MOST's 973 project: 2006CB601002 and 2006CB921300.

* Electronic address: dlffeng@fudan.edu.cn

- [1] B. Dardel *et al.*, Phys. Rev. Lett. **67**, 3144 (1991).
- [2] B. Dardel *et al.*, Europhys. Lett. **19**, 525 (1992).
- [3] K. M. Shen *et al.*, Science **307**, 901 (2005).
- [4] T. Nakagawa *et al.*, Phys. Rev. Lett. **86**, 4854 (2001).
- [5] J. A. Wilson, F. J. Di Salvo and S. Mahajan, Adv. Phys. **24**, 117 (1975).
- [6] D. E. Moncton, J. D. Axe and F. J. Di Salvo, Phys. Rev. Lett. **34**, 734 (1974).
- [7] K. Rossnagel *et al.*, Phys. Rev. B **72**, 121103 (2005).
- [8] W. C. Tonjes *et al.*, Phys. Rev. B **63**, 235101 (2001).
- [9] A. H. Castro Neto, Phys. Rev. Lett. **86**, 4382 (2001).
- [10] T. Yokoya *et al.*, Science **294**, 2518 (2001).
- [11] L. Fang *et al.*, Phys. Rev. B **72**, 014534 (2005).
- [12] This normalization also matches the valence band at higher binding energies reasonably.
- [13] G. Y. Guo and W. Y. Liang, J. Phys. C: Solid State Phys. **20**, 4315 (1987).
- [14] L. Kipp *et al.*, Phys. Rev. Lett. **83**, 5551 (1999).
- [15] H. Ding *et al.*, Phys. Rev. Lett. **78**, 2628 (1997).

- [16] N. Furukawa, T. M. Rice and M. Salmhofer, Phys. Rev. Lett. **81**, 3195 (1998).
- [17] R. L. Barnett *et al.*, Phys. Rev. Lett. **96**, 026406 (2006).
- [18] G. Grüner, *Density Waves in Solids*. (Addison-Wesley Longman, **1994**)
- [19] The same $\alpha = 0.71$ is used for the entire zone, and we have checked that the gap size varies within $\pm 4\%$ against a $\pm 10\%$ change of α .
- [20] T. M. Rice and G. K. Scott Phys. Rev. Lett. **35**, 120 (1975).
- [21] R. Liu *et al.*, Phys. Rev. Lett. **80**, 5762 (1998).
- [22] Th. Straub *et al.*, Phys. Rev. Lett. **82**, 4504 (1999).
- [23] K. Rossnagel *et al.*, Phys. Rev. B **64**, 235119 (2001).
- [24] T. Valla *et al.*, Phys. Rev. Lett. **85**, 4759 (2000).
- [25] T. Valla *et al.*, Phys. Rev. Lett. **92**, 086401 (2004).
- [26] T. P. Devereaux, T. Cuk, Z.-X. Shen and N. Nagaosa, Phys. Rev. Lett. **93**, 117004 (2004).
- [27] D. E. Moncton, J. D. Axe and F. J. Di Salvo, Phys. Rev. B **16**, 801 (1977).
- [28] U. Chatterjee *et al.*, Phys. Rev. Lett. **96**, 107006 (2006).
- [29] K. McElroy *et al.*, Phys. Rev. Lett. **96**, 067005 (2006).
- [30] J. L. Wang and H. Q. Lin, preprint.